Gil-Castell, Ó.; Santiago, Ó.; Pascual-Jose, B.; Navarro, E.; Leo, TJ.; Ribes-Greus, MD. (2020). Performance of sulfonated poly(vinyl alcohol)/graphene oxide polyelectrolytes for direct methanol fuel cells. Energy Technology (Online). 8(7):1-10. https://doi.org/10.1002/ente.202000124

Performance of Sulfonated Poly(Vinyl Alcohol)/Graphene Oxide Polyelectrolytes for Direct Methanol Fuel Cells

O. Gil-Castell[A,B], Ó. Santiago[C,D], B. Pascual-Jose[A], E. Navarro[C], T.J. Leo[D], A. Ribes-Greus[A,*]

[B]Departament d'Enginyeria Química. Escola Tècnica Superior d'Enginyeria. Universitat de València. Av. de la Universitat, s/n, 46100, Burjassot, Spain

[C]Departamento de Mecánica de Fluidos y Propulsión Aeroespacial, ETS Ingeniería Aeronáutica y del Espacio, Universidad Politécnica de Madrid, Plza. Cardenal Cisneros 3, Madrid, 28040, Spain

[D]Departamento de Arquitectura, Construcción y Sistemas Oceánicos y Navales, ETSI Navales, Universidad Politécnica de Madrid, Avda. de la Memoria 4, Madrid, 28040, Spain

[*]Corresponding author:

Prof. Dr. A. Ribes-Greus aribes@ter.upv.es

Performance of Sulfonated Poly(Vinyl Alcohol)/Graphene Oxide Polyelectrolytes for Direct Methanol Fuel Cells

O. Gil-Castell[A,B], Ó. Santiago[C,D], B. Pascual-Jose[A], E. Navarro[C], T.J. Leo[D], A. Ribes-Greus[A],*

Keywords

Fuel cell, polyelectrolyte, membrane, proton exchange, DMFC

Abstract

The use nanotechnology along with the consideration of a functionalization and stabilization approach to the poly(vinyl alcohol) (PVA) was considered useful for the preparation of cost-effective polyelectrolyte membranes. A set of nanocomposite and crosslinked membranes based in PVA/SSA/GO were prepared and analyzed as polyelectrolytes in direct methanol fuel cells (DMFCs). The crosslinking and sulfonation by the use of sulfosuccinic acid (SSA) enhanced the stability and increased the proton conducting sites in the PVA structure. The presence of graphene oxide (GO) augmented the stability, remarkably decreased the methanol crossover and enhanced power density curves. An optimum value for proton conductivity was found for the 0.50%wt of GO proportion, which decreased to higher concentrations of GO. Given the power density curve dependency on both the proton conductivity and the crossover reduction, the performance of these membranes as polyelectrolytes in DMFCs is strictly related to the balance between both factors. Therefore, a proportion of GO of 0.75%wt may assure suitable proton conductivity 3 $mS \cdot cm^{-1}$ and high resistance to methanol permeability, reaching promising power density of 16 $mW \cdot cm^{-2}$ with lower hydration levels.

1. Introduction

The demand for alternative environmentally friendly technologies to reduce the greenhouse gas emissions is nowadays higher than ever before. Fuel cells are one of the most promising technologies thanks to its capacity to convert chemical energy into electricity. Although several

fuels can be used, methanol ranks as one of the best alternatives due to its high fuel energy density, ease of transportation and refilling, and possibility to be obtained from renewable resources [1], [2]. In addition, it does not need bulky tanks, thereby reducing the volume and weight of the entire system. This flexibility of operation places direct methanol fuel cells (DMFC) as a real alternative to traditional energy conversion systems based on fossil fuels, being able to operate alone or in combination with other power electrical devices, such as batteries or supercapacitors. Consequently, this technology might be applicable to several industrial fields, as for instance, transport, energy or consumer electronics [3], [4]. Nevertheless, for this to become a reality there are still several drawbacks that need to be addressed [5], [6].

One of the main challenges DMFCs are facing is the methanol crossover [7]. This phenomenon occurs when methanol moves from the anode to the cathode across the membrane, resulting in a loss of performance. In order to obtain a long-lasting solution, it is necessary to reengineer the membrane. To that purpose, several possibilities are available: modification of Nafion membranes or research on new polymer blends and composites to obtain new materials with optimum properties for fuel cell applications [8]. Concerning research on polymer-based membranes, different alternatives have been proposed in the literature. In particular, membranes based in poly(vinyl alcohol) (PVA) have been reported with high potential for proton exchange polyelectrolytes, as it is a cost-effective and widely available polymer, with great functionalization possibilities and known to be a good methanol barrier, hence being a good candidate to tackle the crossover phenomena that negatively affects DMFC performance [9]–[11]. However, its intrinsic lack of proton conductivity and high water solubility may be disadvantages that must be overcome. The use of crosslinking agents in combination with fillers may be considered to avoid both issues [12]. The combination of PVA and sulfosuccinic acid (SSA), may increase the mechanical properties, diminish swelling related problems and endorse dimensional stability to the polymer matrix [13]. In terms of chemical structure and reaction

mechanism, the crosslinking of PVA and SSA will result in a tridimensional architecture with the generation of ester linkages between both carboxylic cues of SSA and pendant hydroxyl groups of PVA [14]. In the literature, SSA concentration up to 50% has been considered. However, excessive crosslinking and sulfonation of the membranes result in higher rigidity and lower water swelling ability, that may promote cracking in the membranes and impair the proton conduction pathways, respectively [15], [16]. The crosslinking process is usually carried at temperature above 100 ºC, so as thermally promoted esterification is allowed between hydroxyl groups of PVA and carboxylic species of SSA [17]. Moreover, given the absence of ionic species in the PVA structure necessary for the proton transport, the SSA possesses sulfonic functional groups, which are essential to promote proton transport across the membrane. Nevertheless, although reasonable behavior of the PVA/SSA membranes has been reported, it is still far from that of the Nafion® membranes [18]–[22].

In order to improve the performance of PVA/SSA membranes, several alternatives have been proposed in the literature [23]–[25]. Among them, the preparation of composites has received great attention. To such purpose a variety of fillers have been studied such as ceramics (TiO_2, SiO_2, hydroxyapatite), montmorillonite (MMT), silica particles or graphene oxide (GO) [26]–[31]. Among them, graphene oxide (GO) may be a good alternative due to its nanometric scale, and good mechanical, chemical and electrical properties that may provide additional benefits to the membrane. Such is the case as the improvement of the proton conductivity, due to an increase in the surface area between the polymer matrix and the filler, as well as the reduction of the absorption of the fuel solution, which result in lower crossover phenomenon [32]–[37]. In terms of structure, the GO nanoparticles may be enclosed into the above described crosslinked structure, with the possibility of both chemically reaction with SSA molecules, and establishing intermolecular interactions with SSA and PVA by means of hydrogen bonding [38]–[40]. In terms of concentration of GO, percentages above 1.00%wt have been reported to

result in aggregation and agglomeration and difficulties for the GO dispersion in the PVA matrix [41], [42] as well as the loss of proton conductivity [42]–[44].

Therefore, the aim of this work is to evaluate the performance in a DMFC of a series of nanocomposite and crosslinked PVA-based membranes with a 30%wt of SSA as a function of GO concentration (0%, 0.50%, 0.75% and 1.00%wt). For this purpose, the chemical and structural characterization along with the evaluation of the thermal properties and thermo-oxidative stability are essential for the validation of the membrane preparation procedure. Furtherly, the methanol solution absorption and retention ability of the membranes needs to be addressed as an indirect evaluation of the methanol crossover. The characteristic polarization and power density curves and the study of the electric and protonic conductivities may allow understanding the mechanisms governing proton exchange through the polyelectrolyte. The study of these properties should allow elucidating the capacity of these composite membranes for their potential application, avoiding the crossover of methanol and maintaining high power density.

2. Results and Discussion

2.1. Crosslinking and Sulfonation: Surface Morphology and Chemical Structure

The obtained crosslinked membranes were smooth, flat and uniform, which microscopic surface micrographs are shown in **Figure 1**. Non-significant differences in terms of porosity or rugosity were found between M-0 and M-1.00 membranes, so that the presence of GO did not altered the surface flatness. However, submicron grains could be intuited in the membrane containing GO, which may be ascribed to nanoparticles in the surface of the membranes.

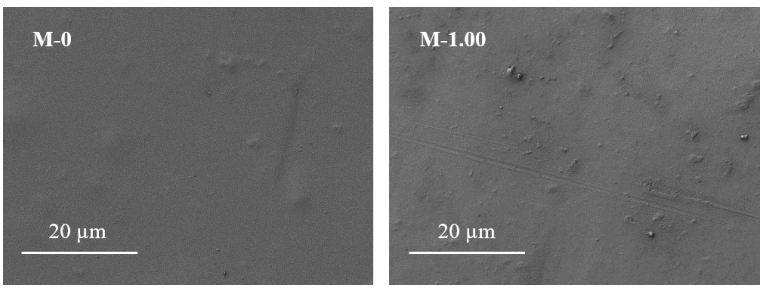

Figure 1. FE-SEM surface micrographs of the M-0 and M-1.00 membranes.

The chemical structure of the membranes was assessed by means of Fourier transform infrared spectroscopy (FT-IR) in order to investigate the existence of crosslinking and sulfonation. The obtained FTIR spectra of the membranes are plotted in **Figure 2** as a function of the GO content.

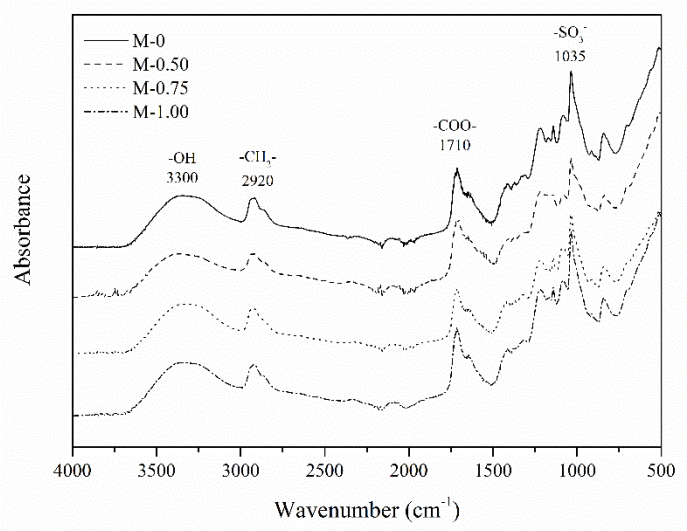

Figure 2. Fourier transform infrared spectra of the membranes.

All the membranes showed the characteristic bands of the PVA, especially those corresponding to the −OH stretching vibration from the intermolecular and intramolecular hydrogen bonds at 3300 cm^{-1} and $-CH_2-$ stretching at 2920 cm^{-1} [45]. Given the thermal crosslinking process with the SSA, the ester bond (−COO−) band was perceived in all cases [16]. The C=O stretching signal at 1710 cm^{-1} was also identified. The use of SSA as sulfonating agent resulted in an intense band around 1035 cm^{-1}, characteristic of the sulfonic groups ($-SO_3H$), that may have overlapped the C−O stretching band, expected at 1050 cm^{-1} [46], [47]. The main bands of the GO, expected at 1615 cm^{-1} for the C=C and at 1220-1250 cm^{-1} for the CO stretching were absent, possibly overlapped by the previously described signals of the PVA and SSA. The low GO content, between 0.50 and 1.00%wt, and the absence of the characteristic GO signals may also be correlated with a good particle dispersion [42]. Altogether, the crosslinking may bring stability to the membrane whereas the sulfonation approach, responsible for introducing proton-

conducting sites in the polymer structure, may improve its protonic conductivity. These features were subsequently evaluated in further sections.

2.2. Thermal Properties and Thermo-Oxidative Stability

The thermal properties of the membranes were assessed by means of differential scanning calorimetry (DSC) and the thermo-oxidative stability was evaluated by means of thermogravimetric analyses (TGA). The results of both techniques were superposed for a proper evaluation of the thermal transitions up to 200 °C. The obtained calorimetric thermograms along with the derivative thermogravimetric curves (DTG) until complete decomposition are plotted in **Figure 3**.

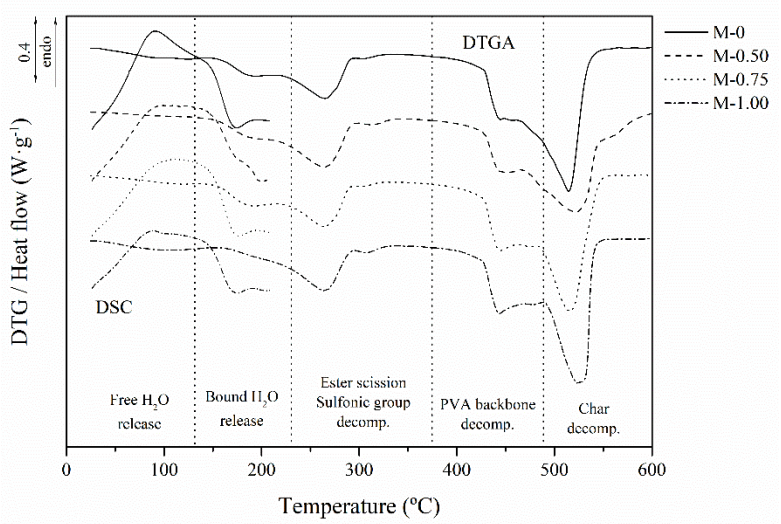

Figure 3. Superposed calorimetric (25-200 °C) and derivative thermogravimetric (25-600 °C) thermograms.

The calorimetric thermograms were characteristic for the PVA/SSA-based crosslinked membranes [18]. An amorphous morphology was suggested given the absence of the melting transitions, as reported before for the PVA-based membranes with a SSA content above 15 %wt [16], [48]. The release of free (<100 °C) and bound water (>100 °C) were perceived as endothermic processes, which enthalpy is plotted in **Figure 4**. The free water is expected to be occupying the free volume available in the membrane structure, while the bound water is

assumed to be interacting by hydrogen bonding with the available sulfonic, hydroxyl and carboxyl groups [49]. Regarding the effect of the nanoparticles, the water release enthalpies decreased as the GO content increased, suggesting the lower ability of the membranes to host water molecules. Moreover, calorimetric thermograms were slightly displaced towards higher temperatures, which would imply stronger membrane-water interactions.

The acquired TGA thermograms revealed a multi-stage thermo-oxidative decomposition. The free and bound water release stages were corroborated along with the ester scission and sulfonic group decomposition, the PVA backbone decomposition and the char degradation [47]. Moreover, when bounded water is released, hydroxyl groups from the PVA molecules may be eliminated, giving as a result polyene structures [16]. The obtained results for these stages are gathered in **Table 1** in terms of the mass loss contribution and peak temperature of the DTG curve. As well, the residue percentage (*R*) after decomposition was included.

Table 1. Characteristic peak temperatures and associated mass loss to the different thermo-oxidative decomposition stages as a function of the membrane composition.

	Free H_2O		**Bounded H_2O**		**Ester/$-SO_3H$**		**PVA backbone**		**Char**		
	T **(°C)**	**Δ*m*** **(%)**	***T*** **(°C)**	**Δ*m*** **(%)**	***T*** **(°C)**	**Δ*m*** **(%)**	***T*** **(°C)**	**Δ*m*** **(%)**	***T*** **(°C)**	**Δ*m*** **(%)**	***R*** **(%)**
M-0	96.18	4.82	189.12	14.56	264.84	16.80	443.31	30.59	514.43	31.00	2.23
M-0.50	93.19	3.12	190.53	13.95	263.99	18.71	444.52	26.95	521.52	34.27	3.00
M-0.75	103.64	3.35	192.44	12.79	264.14	19.49	444.02	29.98	515.51	31.43	2.96
M-1.00	104.35	2.13	-	9.36	264.16	19.04	443.69	28.48	523.96	34.32	3.67

As suggested by the calorimetric analysis, the peak temperatures of the water release were slightly displaced towards higher values and the mass contribution decreased as a function of the GO content. The peak temperature of the ester group scission and the sulfonic group decomposition remained almost constant around 264 °C. However, the mass contribution for this stage slightly increased when GO was incorporated. The degradation of the ester bonds of

the PVA-SSA and SSA-GO molecules may be the responsible for this higher mass contribution. Then, the PVA backbone decomposition occurred around 444 °C. Finally, the char decomposition occurred from 514 °C onwards, with a mass contribution of more than 30%. As expected, the residue varied between 2.23 and 3.67%, being higher as the GO content increased.

For comparison purposes, the water release enthalpy and consequent mass loss step during thermogravimetry are plotted in **Figure 4**. Both parameters decreased as a function of the GO proportion, which highlight the lower water content of the membranes when GO content increased. This observation may be correlated with a more compact structure due to the presence of GO particles, that resulted into a less free volume architecture due to high interaction with PVA and SSA with subsequent less functional group availability for water incorporation [50].

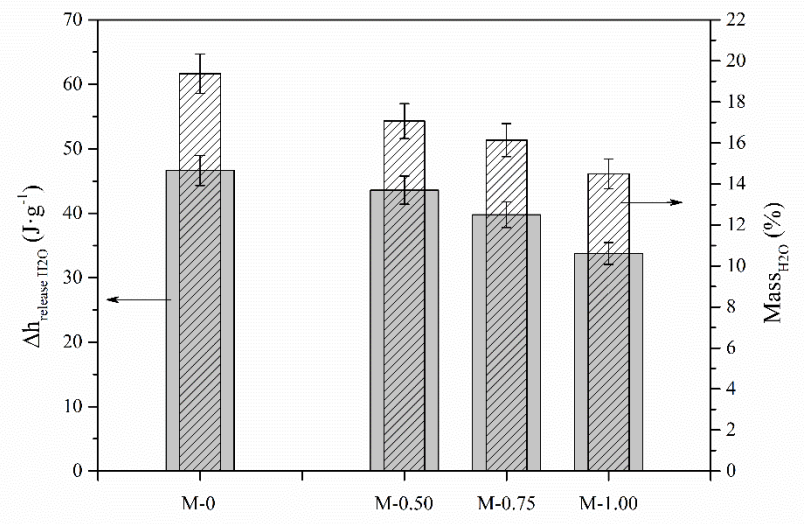

Figure 4. Comparison of the water –free and bounded– release enthalpy (calorimetry) and mass loss (thermogravimetry) as a function of the membrane composition.

2.3. Membrane Stability and Methanol Solution Uptake in Simulated Service Conditions

The membranes were furtherly evaluated by means of the methanol solution uptake at equilibrium. For this purpose, membranes were immersed in a 1 M methanol solution during 65 days. On the one hand, all of them were hydrolytically stable after the assay and no weight loss

due to erosion or fragmentation was found. Indeed, a neat mass increase was found in all cases once reached the equilibrium given the solution incorporation.

The determination of the swelling behavior is important for a satisfactory application as proton exchange membrane, especially in the case of DMFCs where membranes work in direct contact with the methanol solution. The obtained absorption mass percentages (M_s) after 65 days of immersion along with the time to reach the equilibrium are plotted in **Figure 5**.

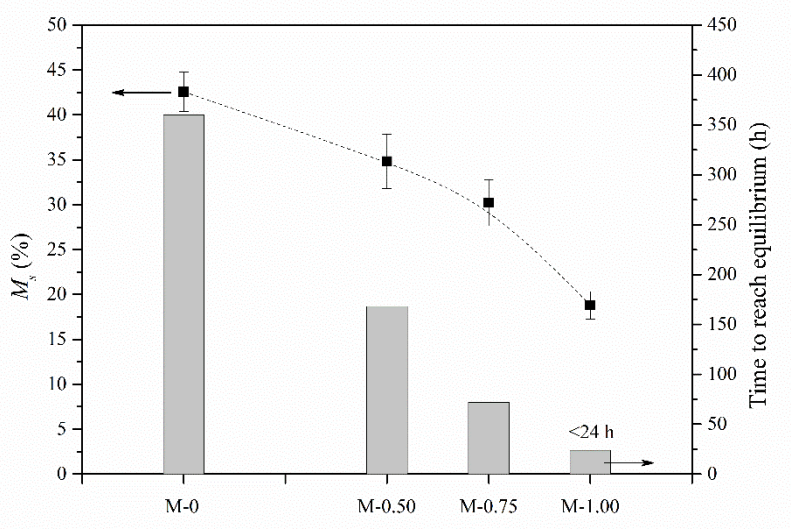

Figure 5. Equilibrium mass percentages at saturation (M_s) as a function of the membrane composition.

In general, membranes became more flexible once saturated given the plasticizing effect of the absorbed solution [17]. The hydrophilic carboxyl, hydroxyl and sulfonic groups of PVA, SSA and GO may have attracted water and methanol molecules. However, the addition of GO considerably decreased the swelling of the membranes. The M_s progressively moved from 42.50% to 34.82% and 30.23% for the M-0.50 and M-0.75, respectively. Then, for the M-1.00, a higher diminution was perceived, reaching the value of 18.79%, the half-mass percentage at saturation of the M-0 membrane. The decrease of the solution uptake may be correlated to the higher matrix-nanoparticle interactions, which have resulted in lower functional sites available for the solution incorporation, as perceived in previous sections [51], [52]. Both chemical and physical interactions reduced the free volume holes and turned the membranes into a more

compact structure. This behavior may be associated to the reduction of the time to reach equilibrium with the addition of GO. Whereas the M-0 continued increasing mass until 350 h, the M-1.00 membrane was saturated in less than 24 h. For the PVA/SSA, it has been reported that the structure of the membranes may change during immersion. Once the hydrophilic functional groups have completely interacted with the dissolution, more water and methanol may be absorbed because of the membrane expansion and swelling. This is the above-mentioned plasticizing effect [17]. Conversely, the GO contributed to modulate the membrane expansion which will result in higher dimensional stability when in contact with the methanol solution during service [37].

For a deeper characterization of the methanol solution uptake, the diffusion coefficient (*D*) was calculated, along with permeability (*P*) and the *n* coefficient for the determination of the diffusion type. The obtained results are gathered in **Table 2**. The solution uptake rate increased for higher GO content, and therefore, the diffusion coefficient (*D*) slightly increased for higher proportions of GO. Although this behavior may be striking, the higher hydrophilicity of the GO nanoparticles may be the responsible of the increase of *D* [53]. Moreover, as a result of the preliminary drying stage before immersion, the avidity of the GO nanoparticles for water molecules may be higher, and therefore, the diffusion coefficient was slightly higher than for the M-0 membrane. Considering the calculated solubility at the equilibrium, and the membrane thickness around 120 μm, the presence of GO nanoparticles diminished the methanol solution permeability (*P*) from $4.94 \cdot 10^{7}$ $cm^2 \cdot s^{-1}$ for the M-0 to $4.48 \cdot 10^{7}$ $cm^2 \cdot s^{-1}$ for the M-1.00 membrane. This behavior was in line with that reported in the literature for the crosslinked PVA/SSA with similar percentages of SSA [48], [54], [55]. In general, permeability to 1 M methanol solution was considerably lower than that of Nafion® 117, reported in the range from 10^{-5} to 10^{-6} $cm^2 \cdot s^{-1}$ [56]–[59].

In terms of diffusion type, a pseudo-Fickian pattern ($n \leq 0.5$) was found in all cases, despite of the presence of GO. This behavior is characteristic for the crosslinked polymers and composites, and responsible of the complex and anomalous penetration pattern of the fluid into the membrane [60]. However, when GO was absent in the composition in the M-0 membrane, the *n* was 0.21, closer to the Case I or Fickian diffusion ($n = 0.5$). The higher concentration of GO in the membrane, the more anomalous diffusion behavior occurred.

Table 2. Diffusion parameter (*D*), *n* coefficient and permeability (*P*) as a function of the membrane composition.

	$D\ 10^6$ ($cm^2 \cdot s^{-1}$)	$P \cdot 10^7$ ($cm^2 \cdot s^{-1}$)	*n*
M-0	1.16	4.94	0.21
M-0.50	1.36	4.73	0.16
M-0.75	1.56	4.70	0.13
M-1.00	1.72	4.48	0.07

Even though diffusion slightly increased as a function of the GO content, the lower absorption at equilibrium along with the more anomalous diffusion type may suggest higher tortuosity and therefore lower methanol crossover across the membrane, as suggested in the literature [61], [62]. This, along with the reported slow water diffusion between graphene oxide layers would result in lower crossover [63]. Moreover, the lower plasticizing effect as a function of the GO percentage can be correlated with a highly interrelated and compact structure with less space for the swelling and generation of hydrophilic channels for the solution diffusion and, thus, reducing crossover, one of the main drawbacks of the membrane development in the DMFC field [36], [64]. Altogether, given the well-known contribution of the water molecules to the proton transport, the consequences of the lower membrane solution uptake and different

diffusion behavior must be investigated in terms of the DMFC performance and the proton conductivity of the membranes.

2.4. Direct Methanol Fuel Cell (DMFC) Performance

The direct methanol fuel cell (DMFC) performance of the membranes was evaluated, which results are plotted in **Figure 6** by means of the polarization and the corresponding power density curves as a function of the GO content and a methanol concentration of 1 M.

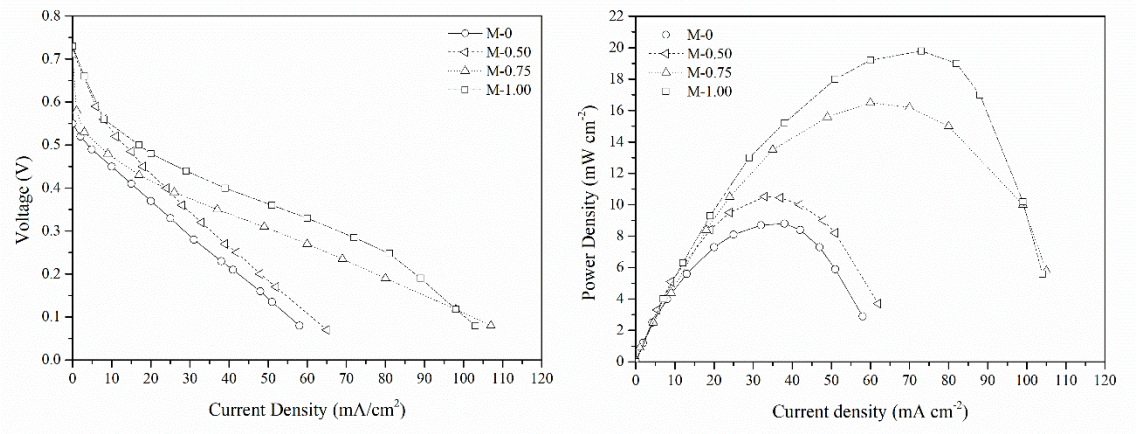

Figure 6. DMFC polarization curves (left) and their corresponding power density curves (right) obtained for a methanol concentration of 1 M.

The performance of the membranes with high GO content (M-0.75 and M-1.00) was considerably higher than that obtained for membranes with low GO content (M-0 and M-0.50). The significant reduction of the methanol crossover found in the previous section is in accordance with the remarkable increase of the OCV in those MEAs with M-0.75 and M-1.00 membranes, as plotted in **Figure 7**. In addition, the crossover reduction may be the responsible for the better power density when GO content increased. As occurred with the uptake ability of methanol solution, (**Figure 5**), this behavior was not linear. In particular, the greatest improvement was found when de GO composition increased from 0.50 to 0.75%wt, which values were close to those reported for Nafion® 117 in 1 M methanol solution at 50 ºC (~30 $mW \cdot cm^2$) [65]. At this point, although the influence of the methanol crossover has been

highlighted on the cell performance, the obtained results suggest that other factors such as the proton conductivity may contribute and therefore must be evaluated.

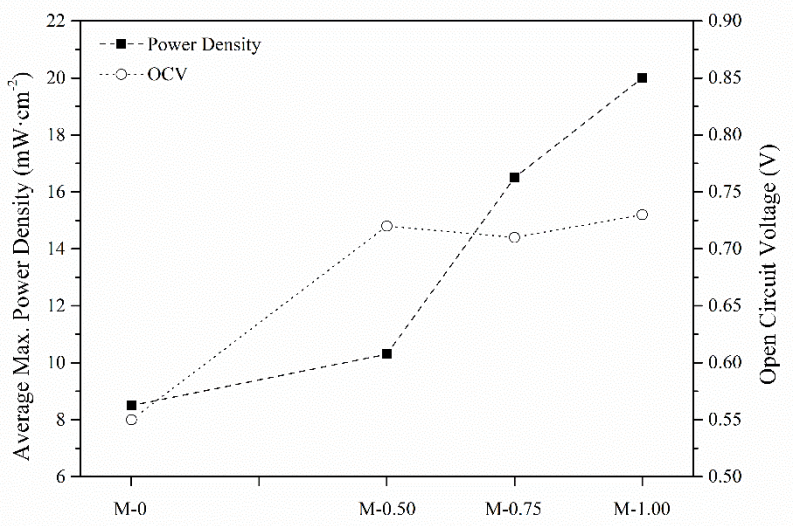

Figure 7. Maximum power densities and open circuit voltages of the crosslinked PVA/SSA and PVA/SSA/GO composite membranes in DMFC at a concentration of 1 M.

2.5. Electrical and Proton Conductivity

Dielectric thermal analysis (DETA) allows to study the electrical (σ_{dc}) and proton conductivity (σ_{prot}), which are key parameters in the reengineering process of a given membrane for DMFC applications [66]. **Figure 8** shows the obtained values for the PVA/SSA/GO membranes in their original (dry) state as a function of temperature.

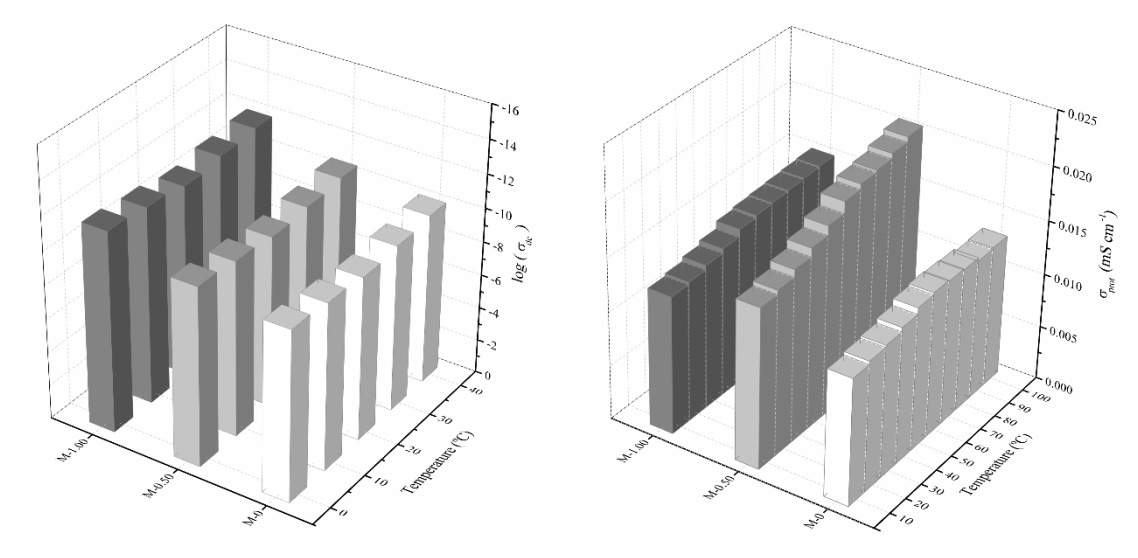

Figure 8. Logarithm of the electrical conductivity (σ_{dc}) (left) and proton conductivity (σ_{prot}) (right) as a function of the membrane composition and temperature, obtained from the membranes in their original (dry) state.

In general, both σ_{dc} and σ_{prot} increased as a function of temperature, due to the higher molecular mobility. The electric conductivity remained between 10^{-10} and 10^{-11} $S \cdot cm^{1}$ for all studied membranes. Given the low electrical conductivity required for DMFC applications, these values can be considered as suitable [8]. Regarding proton conductivity (σ_{prot}), it increased with the addition of GO and a maximum value was found for the M-0.50 membrane. Membranes were furtherly analyzed at the service temperature after being immersed in water during 24 h. **Figure 9** compares the obtained σ_{prot} in the dry and wet states. Significant differences were perceived, including an increase of two orders of magnitude when the membranes were hydrated. This observation is strictly correlated to the contribution of the vehicular mechanism by means of the absorbed water molecules, both free and bound. Again, a maximum was obtained for the M-0.50 membrane. In particular, although this composition revealed a σ_{prot} of 3.06 $mS \cdot cm^{-1}$ at 25 ºC, it was still lower than that of the Nafion® 117 membrane with 37.4 $mS \cdot cm^{-1}$. Even though the proposed membranes are still below the Nafion® performance in terms of proton conductivity, a promising reduction in the methanol solution uptake and permeation coefficient, along with a reasonably good fuel cell behavior with the addition of small proportions of GO

and simple and cost-effective preparation methodology makes these membranes promising candidates for further developments in this field.

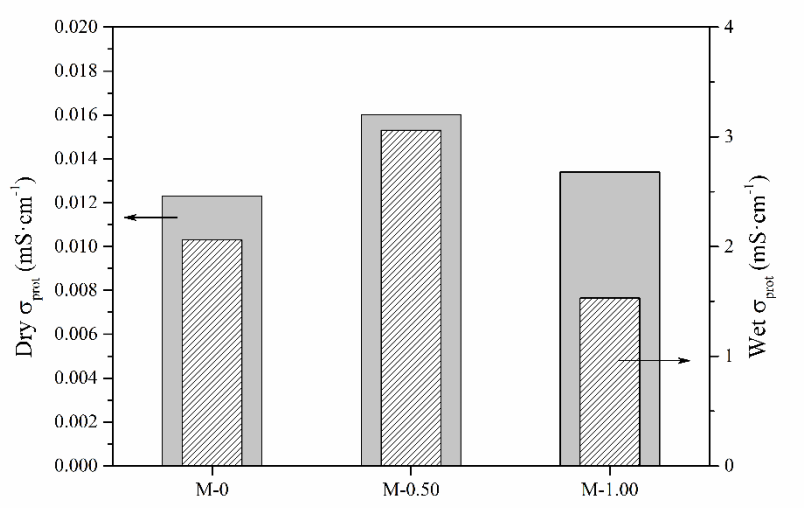

Figure 9. Comparison of the σ_{prot} in the dry and wet states as a function of the membrane composition.

As the proton transfer is understood as a combination of vehicular and Grotthuss mechanisms [67]–[69], the presence of GO in the membrane may have promoted a more compact structure, with lower free volume, in which the ionic sites for proton transport are closer. Thus, less molecules of water are required to proton transfer [51]. However, when GO content increased reached 1.00 %wt, the σ_{prot} considerably decreased. The lower hydration ability of the membranes with high GO content may have reduced the crossover phenomenon found in previous sections but also the contribution of the water molecules to the vehicular proton transport mechanism. In addition, the ionic pathways may have been blocked by GO nanoparticles, which may have reduced the proton hopping mechanism and subsequently the overall proton conductivity [65].

According to the results found in this study, the **Figure 10** schematizes the proposed contribution of the Grotthuss and vehicular proton transport mechanisms and methanol crossover as a function of the GO content in the PVA/SSA/GO membranes.

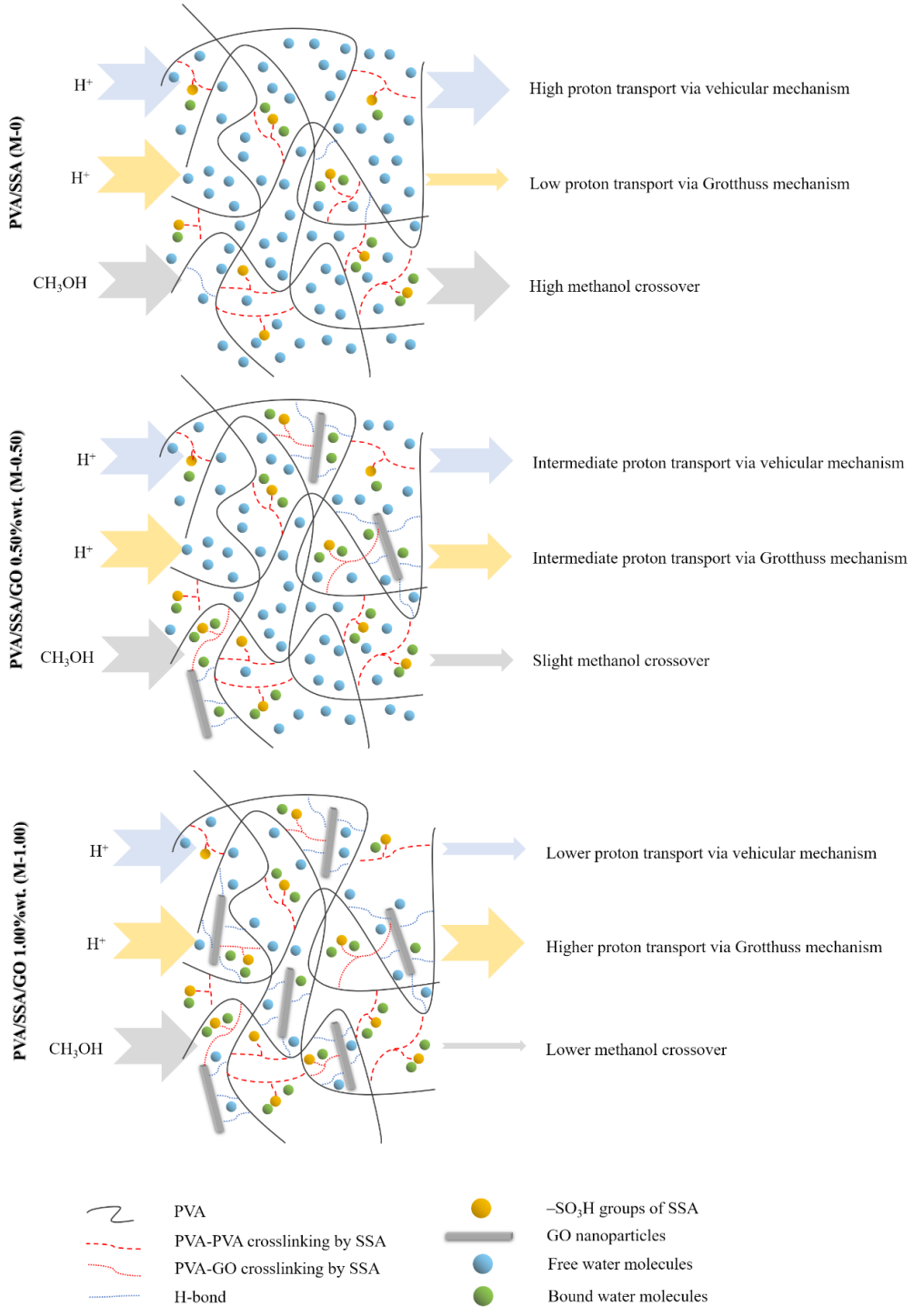

Figure 10. Scheme of the proposed contribution of the Grotthuss and vehicular proton transport mechanisms and methanol crossover as a function of the GO content in the membranes.

3. Conclusions

The prepared nanocomposite and crosslinked membranes based in PVA/SSA/GO may be postulated as a cost-effective alternative for being used as polyelectrolytes in direct methanol fuel cells (DMFCs).

Regardless of the amount of GO, they revealed a non-porous smooth and flat surface along with appropriate thermal stability, flexibility and a low electric conductivity. In terms of performance in DMFC, it was demonstrated that the balance between both the proton conductivity and the ability of the membrane to slow down the crossover process is essential for a successful application. Whereas proton conductivity increases with the inclusion of GO until a percentage of 0.50%wt, the presence of GO in the membranes decreases the absorption of the methanol solution, further as GO content increased.

Better power density performance with GO was achieved. However, a non-linear relationship was defined. Overall, membranes with GO proportion of 0.75%wt combined good proton conductivity and high resistance to methanol permeability and exhibited appropriated behavior with lower hydration levels for being used as polyelectrolytes in DMFCs.

4. Experimental Section

4.1. Materials

Poly(vinyl alcohol) (PVA) with M_n 67 000 g·mol^{-1} (degree of hydrolysis min. 99%), glacial acetic acid (99.8% anhydrous), sulfosuccinic acid (SSA) (70%wt solution in water) were all purchased from Sigma-Aldrich. Methanol from Panreac (99.9% purity) and Millipore water were used. All chemicals were used without further purification.

The graphene oxide (GO) was prepared from graphite powder using the Modified Hummers Method (MHM) [42], [70], [71]. Concisely, graphite powder (<20 μm) was mixed with H_2SO_4 and $NaNO_3$, below 20 °C, after which $KMnO_4$ was progressively added under constant stirring.

Then, the mixture was diluted in distilled water and the temperature increased to 98 °C. To reduce the remaining $KMnO_4$, a H_2O_2 solution 30% was added and the solid phase was washed with HCl 37% and ethanol until neutral pH was reached. Finally, the GO powder was filtered and dried in a vacuum oven at 60 °C. All the reactive used for the GO preparation were purchased from Sigma-Aldrich.

4.2. Membrane Preparation

Nanocomposite membranes based in PVA/SSA/GO were prepared by means of a solvent-casting procedure [72]. First, PVA (5 g) were dissolved in deionized water (100 mL) and magnetically stirred at 90 °C for 8 h. Then, the aqueous solution of SSA was gradually added to the flask in order to achieve a 30%wt_{PVA} and furtherly stirred for 24 h [47]. Afterwards, four identic aliquots of this solution were obtained, which were mixed with GO dispersions, refluxed at 90 °C overnight and finally cooled down to room temperature. The GO dispersions containing the 0.50, 0.75 and 1.00%wt_{PVA} were previously prepared in deionized water (10 mL) and sonicated for 1 h. Finally, the solutions were cast on a Teflon® mold dishes. Once dry, the membranes were cross-linked at 110 °C during 2 h. The membranes were labelled as M-0, M-0.50, M-0.75 and M-1.00, according to the GO percentage with respect to the PVA.

4.3. Membrane Physicochemical Characterization

4.3.1. Field-Emission Scanning Electron Microscopy (FE-SEM)

The surface of the prepared membranes was evaluated by means of Field-emission scanning electron microscopy (FE-SEM). The membranes, previously vacuum dried, were platinum sputter-coated during 10 s using a Leica EM MED020 coater. Surface electronic micrographs were taken in a Zeiss Ultra 55 at 22 ºC with a 1 kV voltage.

4.3.2. Fourier Transform Infrared Spectroscopy (FTIR)

The chemical structure was assessed by means of Fourier transform infrared spectroscopy (FTIR). Analyses were carried out in a Thermo Nicolet 5700 infrared spectrometer with an attenuated total reflectance accessory (ATR). The spectra were collected from 4000 to 400 cm^{-1} at a resolution of 4 cm^{-1} along 64 scans. The spectra of three different locations of the sample were averaged. Backgrounds were collected and results were processed by means of the Omnic® Software.

4.3.3. Differential Scanning Calorimetry (DSC)

The thermal properties were assessed by means of differential scanning calorimetry (DSC) using a Mettler Toledo DSC 822 analyzer. Thermograms were obtained from 25 °C to 220 °C at 10 °C·min^{-1}. All the experiments were run under nitrogen atmosphere (50 mL·min^{-1}). Three consecutive scans of heating, cooling and heating were carried out. Samples were analyzed in triplicates and results were evaluated by means of the STARe® Software.

4.3.4. Thermogravimetric Analysis (TGA)

The thermo-oxidative stability of the membranes was assessed by means of thermogravimetric analysis (TGA) in a Mettler-Toledo TGA 851 analyzer. The samples, with a mass of about 4 mg were introduced in an alumina pans, with capacity of 70 μL, and were analyzed in triplicates from 25 to 800 °C with a heating rate of 10 °C·min^{-1}, under an oxygen atmosphere (50 mL·min^{-1}). Results were analyzed by means of the STARe® Software.

4.4. Membrane Validation

4.4.1. Methanol Solution Absorption

Specimens of 1 cm^2 were preliminarily dried at 30 ºC and vacuum conditions into a Heraeus Vacutherm 6025 oven for 48 h until constant mass, and subsequently immersed into closed vials containing 1 M methanol solution (20 mL) at 50 °C. The change in the mass of the

specimens was evaluated gravimetrically up to saturation according to **Equation (1)** with a Mettler-Toledo XS205 Dual-Range, where m_t refers to the mass measured along immersion and m_0 is the initial mass of the membranes. The aqueous media was replaced weekly during immersion by fresh 1 M methanol solution.

$$M_t(\%) = \frac{m_t - m_0}{m_0} \times 100 \qquad (1)$$

According to the geometric structure of the material under study, the solution to Fick's law for the diffusion evaluation may be different [23]. For the case of a plane sheet geometry, the mass uptake at time t may be designed as M_t and the uptake at the equilibrium as M_{eq}. Therefore, for the earlier stages of solution uptake ($M_t/M_{eq} \leq 0.5$), the Fick's law can be simplified using Stefan's approximation described in **Equation (2)** [73].

$$\frac{M_t}{M_{eq}} = \frac{8}{\pi^{1/2}} \left(\frac{Dt}{l^2}\right)^{1/2} \qquad (2)$$

where D is the diffusion coefficient, t the time of absorption and l is the thickness of the sample. By representing the M_t/M_{eq} ratios as a function of the square root of time, it can be calculated Θ, the slope of the plot. So, the diffusion coefficient (D) can be calculated according to the **Equation (3)**.

$$D = 0.0625\pi l^2 \theta^2 \qquad (3)$$

In order to understand the degree of interaction between the methanol solution and the membrane, it can be calculated the sorption coefficient S using the **Equation (4)**.

$$S = \frac{(m_s - m_0)}{m_0} \qquad (4)$$

where m_p is the membrane initial dry weight and m_s is the weight of the specimen at the equilibrium.

The permeation coefficient (P) can be therefore calculated by combining the diffusion and sorption coefficients in **Equation (5)** [74], [75].

$$P = D \cdot S \qquad (5)$$

In terms of diffusion behavior, it may be considered that, for short times, the **Equation (6)** may be considered that, if linearized applying logarithms as in **Equation (7)**, the slope may allow to obtain the *n* coefficient for the diffusion type evaluation.

$$\frac{M_t}{M_\infty} = K \cdot t^n \qquad (6)$$

$$\log\left(\frac{M_t}{M_\infty}\right) = \log K + n \cdot \log t \qquad (7)$$

4.4.2. Polarization Curve Measurements

To identify the real potential of the synthetized membranes for being used in fuel cells, they were tested by means of membrane electrode assemblies (MEAs) in a single DMFC of 3.8 cm^2 of active area. Before assembling the single cell, membranes were sandwiched between two full wet filter papers for 30 min to hydrate them properly. In order to apply a uniform pressure a ceramic plate was placed on top.

Commercial electrodes from Freudemberg were used to prepare the MEAs, Pt-Ru/C (3 $mg \cdot cm^{-2}$, BC-M100-30F H2315 T10A) for the anode and Pt/C (1 $mg \cdot cm^{-2}$, BC-H225-10F) for the cathode. Thus, after the hydration process, membranes were placed between the electrodes and the set was clamped between two monopolar plates by 4 screws with 2 N·m of torque. Each monopolar plate consists of a stainless steel 316L plate with a parallel-channel flow pattern to supply the reactants.

Membranes with different GO content were tested in the single DMFC. The anode of the cell was supplied with 1 M methanol solutions, at 3 $mL \cdot min^{-1}$, whereas pure humidified oxygen at 50 $mL \cdot min^{-1}$ was continuously provided to the cathode. The polarization curves were acquired at 50 °C and 1 bar oxygen pressure. Before conducting the polarization curve measurement, the single cell was subjected to a thermal conditioning procedure. It consisted in heating the cell at open circuit voltage (OCV) up to the working temperature (50 °C) by means of a heat

exchanger. Polarization curves were obtained keeping each point for 60 s. The polarization curve measurements were performed in a previously reported experimental setup [76].

4.4.3. Dielectric Thermal Analysis (DETA)

The proton and the electric conductivities of the membranes were analyzed by means of dielectric thermal analysis (DETA), using a Spectrometer of Novocontrol Technologies. The response was measured in the frequency range $f = 10^{-1} – 10^{7}$ Hz, at temperatures between -150 to 100 °C. All the measurements were obtained under isothermal conditions by increasing steps of 10 °C. The sample electrode assembly (SEA) consisted in two stainless steel electrodes (20 mm diameter) filled with the sample. The proton conductivity of the polyelectrolytes was calculated according to **Equation (8)**.

$$\sigma_{prot} = \frac{L}{A \cdot R_o} \qquad (8)$$

where L is the thickness of the polyelectrolytes in cm, A the area of the electrode in contact with the membrane in cm^2, and R_0 the protonic resistance in ohms (Ω). The value of R_0 is taken from the Bode plot in the high frequency range, in which the value of log $|Z|$ tends to a non-frequency dependent asymptotic value and the phase angle reaches its maximum value [77].

The electric conductivity (σ_{dc}) was also measured from the **Equation (8)** but with the values of R_0 at low frequencies, where the measured real part of the conductivity reaches a plateau.

Conflict of Interest

The authors declare that there is no conflict of interest regarding the publication of this article.

Acknowledgements

The Spanish Ministry of Economy, Industry and Competitiveness is acknowledged for the projects ENE2017-86711-C3-1-R, ENE2017-86711-C3-2-R, ENE2017-90932-REDT and UPOV13-3E-1947. The Spanish Ministry of Education, Culture and Sports is thanked for the pre-doctoral FPU grant for O. Gil-Castell (FPU13/01916).

Received:

Revised:

Published online:

References

[1] S. Mohanapriya, G. Rambabu, S. Suganthi, S. D. Bhat, V. Vasanthkumar, V. Anbarasu, and V. Raj, "Bio-functionalized hybrid nanocomposite membranes for direct methanol fuel cells," *RSC Adv.*, vol. 6, no. 62, pp. 57709–57721, 2016.

[2] H. Bahrami and A. Faghri, "Review and advances of direct methanol fuel cells: Part II: Modeling and numerical simulation," *J. Power Sources*, vol. 230, pp. 303–320, 2013.

[3] B. C. Ong, S. K. Kamarudin, and S. Basri, "Direct liquid fuel cells: A review," *Int. J. Hydrogen Energy*, vol. 42, no. 15, pp. 10142–10157, 2017.

[4] O. Barbera, A. Stassi, D. Sebastian, J. L. Bonde, G. Giacoppo, C. D'Urso, V. Baglio, and A. S. Aricò, "Simple and functional direct methanol fuel cell stack designs for application in portable and auxiliary power units," *Int. J. Hydrogen Energy*, vol. 41, no. 28, pp. 12320–12329, 2016.

[5] D. S. Falcão, V. B. Oliveira, C. M. Rangel, and A. M. F. R. Pinto, "Review on micro-direct methanol fuel cells," *Renew. Sustain. Energy Rev.*, vol. 34, pp. 58–70, 2014.

[6] X. Li and A. Faghri, "Review and advances of direct methanol fuel cells (DMFCs) part I: Design, fabrication, and testing with high concentration methanol solutions," *J. Power Sources*, vol. 226, pp. 223–240, 2013.

[7] Z. Xia, X. Zhang, H. Sun, S. Wang, and G. Sun, "Recent advances in multi-scale design and construction of materials for direct methanol fuel cells," *Nano Energy*, vol. 65, p. 104048, Nov. 2019.

[8] A. Mahmoud and I. Dincer, "A review on methanol crossover in direct methanol fuel cells: challenges and achievements," *Int. J. ENERGY Res.*, vol. 35, pp. 1213–1228, 2011.

[9] N. W. DeLuca and Y. A. Elabd, "Polymer electrolyte membranes for the direct methanol fuel cell: A review," *J. Polym. Sci. Part B Polym. Phys.*, vol. 44, no. 16, pp. 2201–2225, Aug. 2006.

[10] C. Y. Wong, W. Y. Wong, K. S. Loh, W. R. W. Daud, K. L. Lim, M. Khalid, and R. Walvekar, "Development of Poly(Vinyl Alcohol)-Based Polymers as Proton Exchange Membranes and Challenges in Fuel Cell Application: A Review," *Polym. Rev.*, vol. 60, no. 1, pp. 171–202, Jan. 2020.

[11] O. Gil-Castell, R. Teruel-Juanes, F. Arenga, A. M. Salaberria, M. G. Baschetti, J. Labidi, J. D. Badia, and A. Ribes-Greus, "Crosslinked chitosan/poly(vinyl alcohol)-based polyelectrolytes for proton exchange membranes," *React. Funct. Polym.*, vol. 142, pp. 213–222, Sep. 2019.

[12] N. Shaari and S. K. Kamarudin, "Recent advances in additive-enhanced polymer electrolyte membrane properties in fuel cell applications: An overview," *Int. J. Energy Res.*, vol. 43, no. 7, pp. 2756–2794, Jun. 2019.

[13] D. Dhanapal, M. Xiao, S. Wang, and Y. Meng, "A Review on Sulfonated Polymer Composite/Organic-Inorganic Hybrid Membranes to Address Methanol Barrier Issue for Methanol Fuel Cells," *Nanomaterials*, vol. 9, no. 5, p. 668, Apr. 2019.

[14] C. Y. Tseng, Y. S. Ye, K. Y. Kao, J. Joseph, W. C. Shen, J. Rick, and B. J. Hwang, "Interpenetrating network-forming sulfonated poly(vinyl alcohol) proton exchange membranes for direct methanol fuel cell applications," *Int. J. Hydrogen Energy*, vol. 36, no. 18, pp. 11936–11945, Sep. 2011.

[15] E. Rynkowska, K. Fatyeyeva, S. Marais, J. Kujawa, and W. Kujawski, "Chemically and thermally crosslinked PVA-based membranes: Effect on swelling and transport behavior," *Polymers (Basel).*, vol. 11, no. 11, pp. 7–9, 2019.

[16] J. M. Morancho, J. M. Salla, A. Cadenato, X. Fernández-Francos, P. Colomer, Y. Calventus, X. Ramis, and R. Ruíz, "Thermal analysis of enhanced poly(vinyl alcohol)-based proton-conducting membranes crosslinked with sulfonation agents for direct methanol fuel cells," *J. Appl. Polym. Sci.*, vol. 124, no. S1, pp. E57–E65, Jun. 2012.

[17] M. M. Gomaa, C. Hugenschmidt, M. Dickmann, E. E. Abdel-Hady, H. F. M. Mohamed, and M. O. Abdel-Hamed, "Crosslinked PVA/SSA proton exchange membranes: Correlation between physiochemical properties and free volume determined by positron annihilation spectroscopy," *Phys. Chem. Chem. Phys.*, vol. 20, no. 44, pp. 28287–28299, 2018.

[18] O. Gil-Castell, D. Galindo-Alfaro, S. Sánchez-Ballester, R. Teruel-Juanes, J. D. Badia, and A. Ribes-Greus, "Crosslinked Sulfonated Poly(vinyl alcohol)/Graphene Oxide Electrospun Nanofibers as Polyelectrolytes," *Nanomaterials*, vol. 9, no. 3, p. 397, Mar. 2019.

[19] D. Ebenezer and P. Haridoss, "Effect of crosslinked poly(vinyl alcohol)/sulfosuccinic acid ionomer loading on PEMFC electrode performance," *Int. J. Hydrogen Energy*, vol. 42, no. 7, pp. 4302–4310, 2017.

[20] T. Remiš and J. Kadlec, "Influence of silicon oxide (SiO2) and sulfosuccinic acid (SSA) loading on properties of poly(vinyl alcohol) (PVA) derived composite membranes," *J. Phys. Conf. Ser.*, vol. 1045, no. 1, 2018.

[21] M. S. Tutgun, D. Sinirlioglu, S. U. Celik, and A. Bozkurt, "Investigation of nanocomposite membranes based on crosslinked poly(vinyl alcohol)–sulfosuccinic acid ester and hexagonal boron nitride," *J. Polym. Res.*, vol. 22, no. 4, pp. 1–11, 2015.

[22] N. Kakati, G. Das, and Y. S. Yoon, "Proton-conducting membrane based on epoxy resin-poly(vinyl alcohol)-sulfosuccinic acid blend and its nanocomposite with sulfonated multiwall carbon nanotubes for fuel-cell application," *J. Korean Phys. Soc.*, vol. 68, no. 2, pp. 311–316, 2016.

[23] C. E. Tsai, C. W. Lin, and B. J. Hwang, "A novel crosslinking strategy for preparing poly(vinyl alcohol)-based proton-conducting membranes with high sulfonation," *J. Power Sources*, vol. 195, no. 8, pp. 2166–2173, 2010.

[24] N. Kakati, J. Maiti, G. Das, S. H. Lee, and Y. S. Yoon, "An approach of balancing the ionic conductivity and mechanical properties of PVA based nanocomposite membrane for DMFC by various crosslinking agents with ionic liquid," *Int. J. Hydrogen Energy*, vol. 40, no. 22, pp. 7114–7123, 2015.

[25] Y. H. Chu, J. E. Lim, H. J. Kim, C. H. Lee, H. S. Han, and Y. G. Shul, "Proton conducting silica mesoporous/heteropolyacid-PVA/SSA nanocomposite membrane for polymer electrolyte membrane fuel cell," *Stud. Surf. Sci. Catal.*, vol. 146, pp. 787–790, 2003.

[26] C. C. Yang, W. C. Chien, and Y. J. Li, "Direct methanol fuel cell based on poly(vinyl alcohol)/titanium oxide nanotubes/poly(styrene sulfonic acid) (PVA/nt-TiO2/PSSA) composite polymer membrane," *J. Power Sources*, vol. 195, no. 11, pp. 3407–3415, 2010.

[27] E. Ogungbemi, O. Ijaodola, F. N. Khatib, T. Wilberforce, Z. El Hassan, J. Thompson, M. Ramadan, and A. G. Olabi, "Fuel cell membranes – Pros and cons," *Energy*, vol. 172, pp. 155–172, 2019.

[28] V. R, R. Sundara, and P. Haridoss, "Analysis of crosslinked polyvinyl alcohol membranes with silica fillers in polymer electrolyte membrane fuel cells," *Mater. Res. Express*, vol. 6, no. 10, p. 105526, Aug. 2019.

[29] D. S. Kim, H. B. Park, J. W. Rhim, and Y. M. Lee, "Proton conductivity and methanol transport behavior of cross-linked PVA/PAA/silica hybrid membranes," *Solid State Ionics*, vol. 176, no. 1–2, pp. 117–126, 2005.

[30] J. Maiti, N. Kakati, S. H. Lee, S. H. Jee, and Y. S. Yoon, "PVA nano composite membrane for DMFC application," *Solid State Ionics*, vol. 201, no. 1, pp. 21–26, Oct. 2011.

[31] Z. Zakaria, N. Shaari, and S. K. Kamarudin, "Preliminary Study of Alkaline Direct Ethanol Fuel Cell by Using Crosslinked Quaternized Poly (Vinyl Alcohol)/Graphene Oxide Membrane (Kajian Awal Sel Fuel Etanol Langsung Beralkali Menggunakan Membran Elektrolit Berasaskan Alkohol Polivinil Terkuaternisasi/Grafin Oksida)," *J. Kejuruter.*, vol. 30, no. 2, pp. 219–227, 2018.

[32] Y. Devrim and A. Albostan, "Enhancement of PEM fuel cell performance at higher temperatures and lower humidities by high performance membrane electrode assembly based on Nafion/zeolite membrane," *Int. J. Hydrogen Energy*, vol. 40, no. 44, pp. 15328–15335, 2015.

[33] D. C. Lee, H. N. Yang, S. H. Park, and W. J. Kim, "Nafion/graphene oxide composite membranes for low humidifying polymer electrolyte membrane fuel cell," *J. Memb. Sci.*, vol. 452, pp. 20–28, 2014.

[34] R. P. Pandey, G. Shukla, M. Manohar, and V. K. Shahi, "Graphene oxide based nanohybrid proton exchange membranes for fuel cell applications: An overview," *Adv. Colloid Interface Sci.*, vol. 240, pp. 15–30, 2017.

[35] Y. He, C. Tong, L. Geng, L. Liu, and C. Lü, "Enhanced performance of the sulfonated polyimide proton exchange membranes by graphene oxide: Size effect of graphene oxide," *J. Memb. Sci.*, vol. 458, pp. 36–46, 2014.

[36] T. Yuan, L. Pu, Q. Huang, H. Zhang, X. Li, and H. Yang, "An effective methanol-blocking membrane modified with graphene oxide nanosheets for passive direct methanol fuel cells," *Electrochim. Acta*, vol. 117, pp. 393–397, Jan. 2014.

[37] A. Ammar, A. M. Al-Enizi, M. A. AlMaadeed, and A. Karim, "Influence of graphene oxide on mechanical, morphological, barrier, and electrical properties of polymer membranes," *Arab. J. Chem.*, vol. 9, no. 2, pp. 274–286, Mar. 2016.

[38] H. Beydaghi, M. Javanbakht, and E. Kowsari, "Synthesis and characterization of poly(vinyl alcohol)/Sulfonated graphene oxide nanocomposite membranes for use in proton exchange membrane fuel cells (PEMFCs)," *Ind. Eng. Chem. Res.*, vol. 53, no. 43, pp. 16621–16632, Oct. 2014.

[39] M. Yoo, M. Kim, Y. Hwang, and J. Kim, "Fabrication of highly selective PVA-g-GO/SPVA membranes via cross-linking method for direct methanol fuel cells," *Ionics (Kiel).*, vol. 20, no. 6, pp. 875–886, Dec. 2014.

[40] X. Yang, L. Li, S. Shang, and X. ming Tao, "Synthesis and characterization of layer-aligned poly(vinyl alcohol)/graphene nanocomposites," *Polymer (Guildf).*, vol. 51, no. 15, pp. 3431–3435, 2010.

[41] J. Liang, Y. Huang, L. Zhang, Y. Wang, Y. Ma, T. Guo, and Y. Chen, "Molecular-Level Dispersion of Graphene into Poly(vinyl alcohol) and Effective Reinforcement of their Nanocomposites," *Adv. Funct. Mater.*, vol. 19, no. 14, pp. 2297–2302, Jul. 2009.

[42] C. González-Guisasola and A. Ribes-Greus, "Dielectric relaxations and conductivity of cross-linked PVA/SSA/GO composite membranes for fuel cells," *Polym. Test.*, vol. 67, pp. 55–67, May 2018.

[43] M. S. Kim, I. Jun, Y. M. Shin, W. Jang, S. I. Kim, and H. Shin, "The Development of Genipin-Crosslinked Poly(caprolactone) (PCL)/Gelatin Nanofibers for Tissue

Engineering Applications," *Macromol. Biosci.*, vol. 10, no. 1, pp. 91–100, Jan. 2010.

[44] K. Kim, J. Bae, M. Y. Lim, P. Heo, S. W. Choi, H. H. Kwon, and J. C. Lee, "Enhanced physical stability and chemical durability of sulfonated poly(arylene ether sulfone) composite membranes having antioxidant grafted graphene oxide for polymer electrolyte membrane fuel cell applications," *J. Memb. Sci.*, vol. 525, pp. 125–134, Mar. 2017.

[45] S. Yun, H. Im, Y. Heo, and J. Kim, "Crosslinked sulfonated poly(vinyl alcohol)/sulfonated multi-walled carbon nanotubes nanocomposite membranes for direct methanol fuel cells," *J. Memb. Sci.*, vol. 380, no. 1–2, pp. 208–215, Sep. 2011.

[46] D. Ebenezer, A. P. Deshpande, and P. Haridoss, "Cross-linked poly (vinyl alcohol)/sulfosuccinic acid polymer as an electrolyte/electrode material for H2-O2 proton exchange membrane fuel cells," *J. Power Sources*, vol. 304, pp. 282–292, 2016.

[47] A. Martínez-Felipe, C. Moliner-Estopiñán, C. T. Imrie, and A. Ribes-Greus, "Characterization of crosslinked poly(vinyl alcohol)-based membranes with different hydrolysis degrees for their use as electrolytes in direct methanol fuel cells," *J. Appl. Polym. Sci.*, vol. 124, no. 2, pp. 1000–1011, Apr. 2012.

[48] J. W. Rhim, H. B. Park, C. S. Lee, J. H. Jun, D. S. Kim, and Y. M. Lee, "Crosslinked poly(vinyl alcohol) membranes containing sulfonic acid group: Proton and methanol transport through membranes," *J. Memb. Sci.*, vol. 238, no. 1–2, pp. 143–151, Jul. 2004.

[49] D. S. Kim, H. B. Park, J. W. Rhim, and Y. M. Lee, "Preparation and characterization of crosslinked PVA/SiO2 hybrid membranes containing sulfonic acid groups for direct methanol fuel cell applications," *J. Memb. Sci.*, vol. 240, no. 1–2, pp. 37–48, 2004.

[50] P. K. Maji, "Graphene-Based Polymer Nanocomposites: Materials for Future

Revolution," *MOJ Polym. Sci.*, vol. 1, no. 3, Jun. 2017.

[51] J. X. Leong, W. A. Diño, A. Ahmad, W. R. W. Daud, and H. Kasai, "Increasing the proton conductivity of sulfonated polyether ether ketone by incorporating graphene oxide: Morphology effect on proton dynamics," *Jpn. J. Appl. Phys.*, vol. 57, no. 3, p. 035201, Mar. 2018.

[52] R. Nasser, S. K. Hubadillah, M. H. D. Othman, and A. A. Mohamed Hassan, "Fabrication and Characterization of Low-Cost Poly(Vinyl Alcohol) Composite Membrane for Low Temperature Fuel Cell Application," *J. Appl. Membr. Sci. Technol.*, vol. 22, no. 1, pp. 55–63, 2018.

[53] G. Wang, B. Wang, J. Park, J. Yang, X. Shen, and J. Yao, "Synthesis of enhanced hydrophilic and hydrophobic graphene oxide nanosheets by a solvothermal method," *Carbon N. Y.*, vol. 47, no. 1, pp. 68–72, Jan. 2009.

[54] D. S. Kim, H. B. Park, J. W. Rhim, and Y. M. Lee, "Preparation and characterization of crosslinked PVA/SiO2 hybrid membranes containing sulfonic acid groups for direct methanol fuel cell applications," *J. Memb. Sci.*, vol. 240, no. 1–2, pp. 37–48, Sep. 2004.

[55] S. Shabanpanah, A. Omrani, and M. M. Lakouraj, "Fabrication and characterization of PVA/NNSA/ GLA/nano-silica proton conducting composite membranes for DMFC applications Fabrication and characterization of PVA/NNSA/GLA/nano-silica proton conducting composite membranes for DMFC applications," 2019.

[56] D. T. Hallinan and Y. A. Elabd, "Diffusion and Sorption of Methanol and Water in Nafion Using Time-Resolved Fourier Transform Infrared-Attenuated Total Reflectance Spectroscopy," 2007.

[57] H. Ahmad, S. K. Kamarudin, U. A. Hasran, and W. R. W. Daud, "Overview of hybrid

membranes for direct-methanol fuel-cell applications," *Int. J. Hydrogen Energy*, vol. 35, no. 5, pp. 2160–2175, Mar. 2010.

[58] Z. Wu, G. Sun, W. Jin, H. Hou, and S. Wang, "A model for methanol transport through Nafion® membrane in diffusion cell," *J. Memb. Sci.*, vol. 325, no. 1, pp. 376–382, Nov. 2008.

[59] L. Chaabane, L. Dammak, D. Grande, C. Larchet, P. Huguet, S. V. Nikonenko, and V. V. Nikonenko, "Swelling and permeability of Nafion®117 in water-methanol solutions: An experimental and modelling investigation," *J. Memb. Sci.*, vol. 377, no. 1–2, pp. 54–64, Jul. 2011.

[60] D. De Kee, Q. Liu, and J. Hinestroza, "Viscoelastic (Non-Fickian) Diffusion," *Can. J. Chem. Eng.*, vol. 83, no. 6, pp. 913–929, May 2008.

[61] Y. Cui, S. I. Kundalwal, and S. Kumar, "Gas barrier performance of graphene/polymer nanocomposites," *Carbon N. Y.*, vol. 98, pp. 313–333, Mar. 2016.

[62] Z. Zakaria, S. K. Kamarudin, and S. N. Timmiati, "Influence of Graphene Oxide on the Ethanol Permeability and Ionic Conductivity of QPVA-Based Membrane in Passive Alkaline Direct Ethanol Fuel Cells," *Nanoscale Res. Lett.*, vol. 14, 2019.

[63] R. Devanathan, D. Chase-Woods, Y. Shin, and D. W. Gotthold, "Molecular Dynamics Simulations Reveal that Water Diffusion between Graphene Oxide Layers is Slow," *Sci. Rep.*, vol. 6, no. 1, pp. 1–8, Jul. 2016.

[64] H.-C. Chien, L.-D. Tsai, C.-P. Huang, C. Kang, J.-N. Lin, and F.-C. Chang, "Sulfonated graphene oxide/Nafion composite membranes for high-performance direct methanol fuel cells," *Int. J. Hydrogen Energy*, vol. 38, no. 31, pp. 13792–13801, Oct. 2013.

[65] S. Al-Batty, C. Dawson, S. P. Shanmukham, E. P. L. Roberts, and S. M. Holmes,

"Improvement of direct methanol fuel cell performance using a novel mordenite barrier layer," *J. Mater. Chem. A*, vol. 4, no. 28, pp. 10850–10857, Jul. 2016.

[66] R. Riande, E., Diaz-Calleja, *Electrical Properties of Polymers.* Boca Raton: CRC Press., 2004.

[67] N. Agmon, "The Grotthuss mechanism," *Chem. Phys. Lett.*, vol. 244, no. 5–6, pp. 456–462, Oct. 1995.

[68] K.-D. Kreuer, A. Rabenau, and W. Weppner, "Vehicle Mechanism, A New Model for the Interpretation of the Conductivity of Fast Proton Conductors," *Angew. Chemie Int. Ed. English*, vol. 21, no. 3, pp. 208–209, Mar. 1982.

[69] K. D. Kreuer, S. J. Paddison, E. Spohr, and M. Schuster, "Transport in proton conductors for fuel-cell applications: Simulations, elementary reactions, and phenomenology," *Chem. Rev.*, vol. 104, no. 10, pp. 4637–4678, Oct. 2004.

[70] W. S. Hummers and R. E. Offeman, "Preparation of Graphitic Oxide," *J. Am. Chem. Soc.*, vol. 80, no. 6, pp. 1339–1339, 1958.

[71] L. Shahriary and A. a. Athawale, "Graphene Oxide Synthesized by using Modified Hummers Approach," vol. 02, no. 01, pp. 58–63, 2014.

[72] C. Bao, Y. Guo, L. Song, and Y. Hu, "Poly(vinyl alcohol) nanocomposites based on graphene and graphite oxide: a comparative investigation of property and mechanism," *J. Mater. Chem.*, vol. 21, no. 36, p. 13942, 2011.

[73] P. Neogi, *Diffusion in Polymers*, vol. 32. Marcel Dekker, 1996.

[74] M. Mulder, *Basic principles of membrane technology*. Kluwer Academic, 1991.

[75] J. Comyn, *Polymer permeability*. Dordrecht: Springer Netherlands, 1985.

[76] T. J. Leo, M. A. Raso, E. Navarro, E. S. De La Blanca, M. Villanueva, and B. Moreno,

"Response of a direct methanol fuel cell to fuel change," *Int. J. Hydrogen Energy*, vol. 35, no. 20, pp. 11642–11648, 2010.

[77] X. Qian, N. Gu, Z. Cheng, X. Yang, E. Wang, and S. Dong, "Methods to study the ionic conductivity of polymeric electrolytes using a.c. impedance spectroscopy," *J. Solid State Electrochem.*, vol. 6, no. 1, pp. 8–15, 2001.

ANNEX. OPEN ACCESS POLICIES

WILEY-VCH

COPYRIGHT TRANSFER AGREEMENT

Date: _____ Contributor name: _____

Contributor address: _____

Manuscript number (if available): _____

Re: Manuscript entitled _____

_____ (the "Contribution")

for publication in _____ (the "Journal")

published by Wiley-VCH Verlag GmbH & Co. KGaA ("Wiley-VCH").

Dear Contributor(s):
Thank you for submitting the Contribution for publication. In order to expedite the editing and publishing process and enable Wiley-VCH to disseminate the Contribution to the fullest extent, we need to have this Copyright Transfer Agreement signed and returned as directed in the Journal's instructions for authors as soon as possible. If the Contribution is not accepted for publication, or if the Contribution is subsequently rejected, this Agreement shall be null and void. **Publication cannot proceed without a signed copy of this Agreement.**

A. RIGHTS GRANTED

1. The Contributor hereby grants to Wiley-VCH for the duration of the statutory term of copyright protection, the full and exclusive rights comprised in the Contribution including but not limited to the right to publish, republish, transmit, sell, distribute, store and process in electronic media of any kind, include in document delivery services and otherwise use the Contribution in whole or in part in electronic and print editions of the Journal and in derivative works throughout the world, in all languages and in all media of expression now known or later developed, and to license or permit others to do so.

2. Reproduction, posting, transmission or other distribution or use of the final Contribution in whole or in part in any medium by the Contributor as permitted by this Agreement requires a citation to the Journal and an appropriate credit to Wiley-VCH as Publisher, suitable in form and content as follows: (Title of Article, Author, Journal Title and Volume/Issue Copyright © [year] copyright owner as specified in the Journal).

3. Please note that Wiley-VCH reserves the right to require changes to the Contribution, including changes to the length of the Contribution, as a condition of acceptance.

4. Please note that Wiley-VCH reserves the right, notwithstanding acceptance, not to publish the Contribution if for any reason such publication would in the reasonable judgement of Wiley-VCH, result in legal liability or violation of journal ethical practices.

B. RETAINED RIGHTS

Notwithstanding the above, the Contributor or, if applicable, the Contributor's Employer, retains all proprietary rights other than copyright, such as patent rights, in any process, procedure or article of manufacture described in the Contribution.

C. PERMITTED USES BY CONTRIBUTOR

1. Submitted Version. Wiley-VCH licenses back the following rights to the Contributor in the version of the Contribution as originally submitted for publication:

a. After publication of the final article, the right to self-archive on the Contributor's personal intranet page or in the Contributor's institution's/employer's institutional intranet repository or archive. The Contributor may not update the submission version or replace it with the published Contribution. The version posted must contain a legend as follows: This is the pre-peer reviewed version of the following article: FULL CITE, which has been published in final form at [Link to final article].

b. The right to transmit, print and share copies with colleagues.

2. Accepted Version. Reuse of the accepted and peer-reviewed (but not final) version of the Contribution shall be by separate agreement with Wiley-VCH. Wiley-VCH has agreements with certain funding agencies governing reuse of this version. The details of those relationships, and other offerings allowing open web use are set forth at the following website: http://www.wiley.com/go/funderstatement. NIH grantees should check the box at the bottom of this document.

3. Final Published Version. Wiley-VCH hereby licenses back to the Contributor the following rights with respect to the final published version of the Contribution:

a. Copies for colleagues. The personal right of the Contributor only to send or transmit individual copies of the final published version to colleagues upon their specific request provided no fee is charged, and further-provided that there is no systematic distribution of the Contribution, e.g. posting on a listserve, website or automated delivery. For those Contributors who wish to send high-quality e-prints, purchase reprints, or who wish to distribute copies more broadly than allowed hereunder (e.g. to groups of colleagues or mailing lists), please contact the publishing office.

b. Re-use in other publications. The right to re-use the final Contribution or parts thereof for any publication authored or edited by the Contributor (excluding journal articles) where such re-used material constitutes less than half of the total material in such publication. In such case, any modifications should be accurately noted.

c. Teaching duties. The right to include the Contribution in teaching or training duties at the Contributor's institution/place of employment including in course packs, e-reserves, presentation at professional conferences, in-house training, or distance learning. The Contribution may not be used in seminars outside of normal teaching obligations (e.g. commercial seminars). Electronic posting of the final published version in connection with teaching/training at the Contributor's institution/place of employment is permitted subject to the implementation of reasonable access control mechanisms, such as user name and password. Posting the final published version on the open Internet is not permitted.

d. Oral presentations. The right to make oral presentations based on the Contribution.

4. Article Abstracts, Figures, Tables, Data Sets, Artwork and Selected Text (up to 250 words).

a. Contributors may re-use unmodified abstracts for any non-commercial purpose. For on-line uses of the abstracts, Wiley-VCH encourages but does not require linking back to the final published versions.

b. Contributors may re-use figures, tables, data sets, artwork, and selected text up to 250 words from their Contributions, provided the following conditions are met:

(i) Full and accurate credit must be given to the Contribution.
(ii) Modifications to the figures, tables and data must be noted. Otherwise, no changes may be made.
(iii) The reuse may not be made for direct commercial purposes, or for financial consideration to the Contributor.
(iv) Nothing herein shall permit dual publication in violation of journal ethical practices.

CTA-VCH